Novel Intermetallic Compound UFe_5Si_3: A New Room-Temperature Magnet with an Original Atomic Arrangement

David Berthebaud,[†] Antonio P. Gonçalves,[‡] Olivier Tougait,*[,†] Michel Potel,[†] Elsa B. Lopes,[‡] and Henri Noël[†]

Laboratoire de Chimie du Solide et Matériaux, UMR CNRS 6226, Université de Rennes 1, 263 Avenue de Général Leclerc, 35042 Rennes, France, and Departemento de Química, Instituto Tecnológico e Nuclear/ CFMC-UL, P-2686-953 Sacavém, Portugal

Received April 5, 2007. Revised Manuscript Received April 25, 2007

The new compound UFe_5Si_3 was prepared by rapid solidification of the melt using a splat cooling technique, followed by annealing at 1173 K for 10 days. Its crystal structure was determined ab initio from powder X-ray diffraction data. It crystallizes in the tetragonal space group *P4*/*mmm*, with lattice parameters at room temperature of $a = 3.9298(3)$ Å and $c = 7.7133(6)$ Å. The structure of UFe_5Si_3, which is new among intermetallic compounds, can be viewed as built up from an infinite three-dimensional framework of Fe and Si atoms defining along the *a* direction, tunnels of hexagonal sections, where the U atoms lie. Alternating and direct current magnetic measurements reveal that UFe_5Si_3 behaves as a hard ferromagnet with a Curie temperature of about 310 K. Measurements on magnetically oriented powder suggest that UFe_5Si_3 has a uniaxial anisotropy with *c* as the easy axis. The electrical resistivity decreases monotonously with decreasing temperature suggesting no other magnetic transition below 300 K. In line with this metallic behavior the thermal variation of the thermoelectric power remains of the order of several μV/K. A maximum around 60 K with a value of 12 μV/K can be ascribed to Kondo interactions and/or crystalline electrical field effects.

Introduction

There are numerous iron-rich intermetallic compounds, but these of important interest in magnetism involve the *f*-transition elements (R). Typically, the iron lattice through the Fe−Fe exchange directly impacts on the value of the Curie temperature whereas the *f* metal through the R−Fe interactions governs the coercivity. From this base, a progressive step of the investigation of hard-ferromagnetic materials was to place in these compounds uranium, which is known to enhance tremendously the value of the total anisotropy. In this respect, the binary compound UFe_2,[1−4] the ternary compounds $UFe_{10}M_2$ with M = Si and Mo[5−10] and the solid solutions $U_2Fe_{17-x}M_x$ with M = Al, Si, and Ge[6,11−15] were thoroughly studied. These systems are extremely complex as a result of the high degree of delocalization of the U 5f electrons that can directly hybridize with the 3d electrons.[16] Indeed, in the three above-mentioned cases, a strong hybridization between U 5f electrons and Fe 3d electrons occurs and creates on the U atoms an orbital and spin moment of the same magnitude, but they are antiparallely coupled, resulting to a mutual cancellation of these contributions. Therefore, the net magnetic moment of the U sublattice is negligible in these phases, and no ferromagnet with high coercive field has been found in U and Fe systems to date.

Another consequence of the strong hybridization between U 5f and Fe 3d wave functions is the reduction up to the cancellation of the magnetic moment borne by the iron atoms. The ternary phases of the U−Fe−Si system can be considered as typical examples. This ternary system which has been extensively studied comprises nine intermediate phases. Beside $UFe_{10}Si_2$[5] and $U_2Fe_{17-x}Si_x$ with $3.3 < x < 4.5$[17] which

* Corresponding author. Tel.: ++ 33 2 23 23 57 40. Fax: ++ 33 2 23 23 67 99. E-mail: tougait@univ-rennes1.fr.
[†] Université de Rennes 1.
[‡] Instituto Tecnológico e Nuclear/CFMC-UL.

(1) Wulff, M.; Lebech, B.; Delapalme, A.; Lander, G. H.; Rebizant, J.; Spirlet, J. C. *Physica B* **1989**, *156*−*157*, 836−838.
(2) Paolasini, L.; Caciuffo, R.; Roessli, B.; Lander G. H. *Physica B* **1997**, *241*−*243*, 681−683.
(3) Andreev, A. V.; Levitin, R. Z. *J. Alloys Compd.* **2002**, *337*, 18−24.
(4) Okane, T.; Takeda Y.; Fujimori, S.-i.; Terai, K.; Saitoh, Y.; Muramatsu, Y.; Fujimori, A.; Haga, Y.; Yamamoto, E.; Ōnuki, Y. *Physica B* **2006** *378*−*380*, 959−960.
(5) Suski, W.; Baran, A.; Mydlarz, T. *Phys. Lett. A* **1989**, *136*, 89−91.
(6) Berlureau, T.; Chevalier, B.; Fournes, L.; Etourneau, *J. Mater. Lett.* **1989**, *9*, 21−23.
(7) van Engelen, P. P. J.; Buschow, K. H. J. *J. Magn. Magn. Mater.* **1990**, *84*, 47−51.
(8) Andreev, A. V.; Suski, W.; Baranov. *J. Alloys Compd.* **1992**, *187*, 293−298.
(9) Estrela, P.; Godinho, M.; Goncalves, A. P.; Almeida, M.; Spirlet, J. C. *J. Alloys. Compd.* **1995**, *230*, 35−41.
(10) Brück, E.; Nakotte, H.; Klaasse, J. C. P.; de Boer, F. R.; Buschow, K. H. J. *J. Magn. Magn. Mater.* **1998**, *177*−*181*, 45−46.
(11) Berlureau, T.; Gravereau, P.; Chevalier, B.; Etourneau, J. *J. Solid State Chem.* **1993**, *104*, 328−37.
(12) Chevalier, B.; Rogl, P.; Etourneau, J. *J. Solid State Chem.* **1995**, *115*, 13−17.
(13) Andreev, A. V.; Homma, Y.; Shiokawa, Y. *Physica B* **2002**, *319*, 208−219.
(14) Andreev, A. V.; Homma, Y.; Shiokawa, Y. *J. Magn. Magn. Mater.* **2003**, *258*−*259*, 500−503.
(15) Gonçalves, A. P.; Noël, H.; Waerenborgh, J. C.; Almeida, M. *Chem. Mater.* **2002**, *14*, 4219−4228.
(16) Paolasini, L.; Lander, G. H.; Shapiro, S. M.; Caciuffo, R.; Lebech, B.; Regnault, L.-P.; Roessli, B.; Fournier, J.-M. *Phys. Rev. B* **1996**, *54*, 7222−7232.
(17) Chevalier, B.; Berlureau, T.; Gravereau, P.; Fournes, L.; Etourneau, J. *Solid State Commun.* **1994**, *90*, 571−573.

10.1021/cm070943w CCC: $37.00
Published on Web 06/19/2007

order ferromagnetically at high temperature, $U_{1.2}Fe_4Si_{9.7}$[18] is the only compound showing Curie−Weiss behavior, with an effective magnetic moment of 2.4 μB/U. This value is significantly reduced from the free ion values of 3.62 and 3.58 μB/U for U^{3+} and U^{4+}, respectively, and also suggests that the local magnetic moment carried by the Fe atoms is negligible. All other reported phases, U_2FeSi_3,[19] UFeSi,[20] U_2Fe_3Si,[21] $U_3Fe_2Si_7$,[22] $U_2Fe_3Si_5$,[23] and UFe_2Si_2,[24] exhibit magnetic behavior that are governed by itinerant electrons. In this situation, investigation of systems combining U and Fe to find new ferromagnets with high corecivity and high anisotropy appears as a tricky task. However, considering that the manifestation of unexpected phenomena often occurs at the verge between antagonist features, it was attempted to map the strength of the U 5f−Fe 3d hybridization within the U−Fe−Si ternary system by a careful examination of the electronic properties of the intermediate phases. During these systematic studies, the new intermediate phase UFe_5Si_3 was evidenced. In this paper, we report on the synthesis, the structural characterization by X-ray powder diffraction, the investigation of the magnetic properties (alternating current (ac) and direct current (dc) magnetization) and transport properties (thermopower and resistivity) of this new compound.

Experimental Section

Synthesis. The starting materials were uranium turnings (nuclear grad), iron pieces (Strem, 5N), and silicon (Strem, 6N). Samples of the new phase UFe_5Si_3 used for the structural characterization by the Rietveld method and the measurements of the physical properties were prepared by splat-cooling using an Edmund Buehler device followed by heat-treatment. The initial stage of this experimental synthesis was to prepare bulk materials with the proper composition by using the typical arc-melting technique. During the splat-cooling step a free falling droplet of about 250 mg melted by the arc is pressed to a thin plate between two Cu pistons that are shot against each other at high velocity. The alloy cooling rate is approximately 10^6 K/s. The resulting discs have a diameter of about 25 mm and a thickness of about 200 μm. These samples were then wrapped into a Mo foil and introduced in an evacuated silica tube which was sealed under a residual atmosphere of argon. The ampoule was heat treated at 1173 K for 10 days and cooled down to room temperature with a rate of 100 K/h. From these discs a 3 mm^2 sample was cut for metallographic and chemical analyses carried out with the help of a 6400-JSM scanning electron microscope equipped with a Oxford Link-Isis spectrometer. The pieces were embedded in resin and polished using SiC paper and diamond paste with granulometry down to 1 μm. A thin layer of gold was deposited on their surfaces. The remaining part of the discs was ground into powder using ball milling.

Table 1. Conditions of X-ray Data Collection for UFe_5Si_3

diffractometer	Bruker AXS D8-Advance
angular range (°2θ)	20−110
step size (°2θ)	0.013 (from 20° to 77°) 0.016 (from 77° to 110°)
scan step time (s)	66.469 (from 20° to 77°) 90.420 (from 77° to 110°)
detector	SOL-X
measurement temperature (K)	293
radiation type	Cu Kα_1 (1.5406 Å)

Powder X-ray Diffraction. The crystalline quality and the identification of the phases as well as the alignment of the powder under applied magnetic field were checked by X-ray powder diffraction techniques, using an Inel CPS 120 diffractometer working with a Co Kα radiation. To obtain patterns of rather good quality, an amount of more than 100 mg of powder and an acquisition time of 1200 s were required. The powder X-ray diffraction pattern used for the structure determination and the Rietveld refinements was collected at room temperature using a Bruker-D8 diffractometer ($\theta-\theta$ Bragg−Brentano geometry), working with a monochromatic Cu Kα_1 radiation (λ = 1.540 56 Å) obtained with an incident-beam curved Ge-monochromator. The diffracted beams were collected with a sol-X detector (energy dispersive detector). The experimental conditions were $10° \leq 2\theta \leq 77°$, $\Delta 2\theta = 0.013°$, and a 66.469 s counting time per point and $77° < 2\theta \leq 105°$, $\Delta 2\theta = 0.016°$, and 90.420 s counting time per point. Data were then normalized to a constant acquisition time, and count esd's were (estimation of standard deviation) calculated. The Rietveld refinements were performed with the help of the FULLPROF[25] program included in the WinPLOTR[26] package. Additional details about the data collection and the Rietveld refinement are given in Table 1.

Physical Measurements. The electrical resistivity was measured in a closed-cycle refrigerator in the 18−300 K temperature range using the four-probe ac method. The thermoelectric power was measured relative to gold by a slow ac technique (10^{-2} Hz), with a thermal gradient of 1 K, in a homemade apparatus similar to the one previously described by Chaikin and Kwak[27]

The ac susceptibility measurements were carried out on a Lakeshore susceptometer in the temperature range 80−320 K with an applied field of 1 Oe, oscillating at 250, 500, and 1000 Hz. dc magnetic measurements were carried out using a Quantum Design MPMS-5 SQUID magnetometer. Zero field cooled (ZFC) and field cooled (FC) data were collected in the temperature range 1.7−350 K with applied fields of 5000 Oe. The hysteresis cycle was measured at 5 K in increasing and decreasing magnetic fields up to 50 kOe.

A few milligrams (4-5 mg) of the free powder was sucked using cryogenic varnish on a diamagnetic support under an applied field of 12 kOe at ambient temperature to orient the crystallites on their easiest magnetization direction. Magnetization as a function of a magnetic field applied parallel and perpendicular to the easy direction of the oriented powder was measured at 5 K.

Results

Synthesis. The existence of this new phase was revealed on heat-treated samples with starting compositions in the

(18) Noguchi, S.; Okuda, K.; Abliz, M; Goto, K.; Kindo, K.; Haga, Y.; Yamamoto, E.; Onuki, Y. *Physica B* **1998**, *246−247*, 456−459.
(19) Kaczorowski, D.; Noel, H. *J. Phys.: Condens. Matter* **1993**, *5*, 9185−9195.
(20) Andreev, A. V.; Honda, F.; Sechovsky, V.; Divis, M.; Izmaylov, N.; Chernyavski, O.; Homma, Y.; Shiokawa, Y. *J. Alloys Compd*. **2002**, *335*, 91−94.
(21) Berthebaud, D.; et al. Unpublished results.
(22) Aliev, F. G.; Aksel'rud, L. G.; Kozyr'kov, V. V.; Moshchalkov, V. V. *Fiz. Tverd. Tela* **1988**, *30*, 1278−1281.
(23) Hickey, E.; Chevalier, B.; Gravereau, P.; Etourneau, J. *J. Magn. Magn. Mater.* **1990**, *90−91*, 501−502.
(24) Szytula, A.; Slaski, M.; Dunlap, B.; Sungaila, Z.; Umezawa, A. *J. Magn. Magn. Mater.* **1988**, *75*, 71−72.
(25) Rodriguez-Carvajal, J. FULLPROF: A program for Rietveld refinement and pattern matching analyses. *Abstracts of the satellite meeting on powder diffraction of the XVth congress of the International Union of Crystallography*, Toulouse, France, 1990, p.127.
(26) Roisnel, T.; Rodriguez-Carvajal, J. *Mater. Sci. Forum* **2001**, *378−381*, 118 (Proceedings of the European Powder Diffraction Conference (EPDIC 7)).
(27) Chaikin, P. M.; Kwak, J. F. *Rev. Sci. Instrum.* **1975**, *46*, 218.

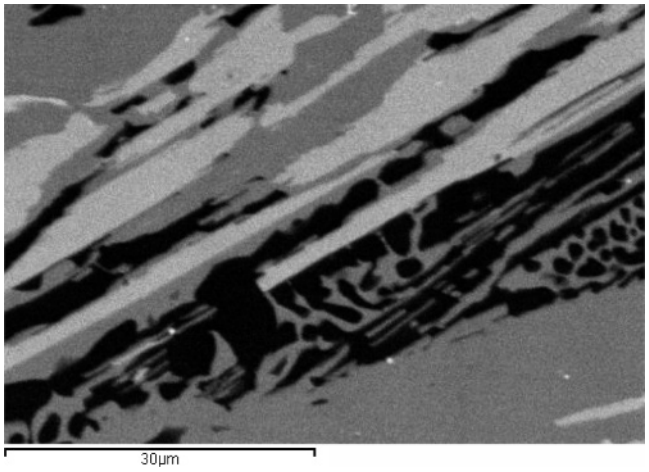

Figure 1. EDS-SEM image of a UFe_5Si_3 sample synthesized by arc-melting followed by annealing at 900 °C. UFe_2Si_2 (gray). UFe_5Si_3 (dark gray). Fe_3Si (black).

section $UFe_2Si_2-U_2Fe_9Si_3-Fe_3Si$ of the ternary diagram. The scanning electron microscopy−energy dispersive spectroscopy (SEM-EDS) showed three thermodynamically stable phases having a composition in agreement with the formulas UFe_2Si_2, Fe_3Si, and UFe_5Si_3. The X-ray diffraction pattern after subtracting the contribution of UFe_2Si_2 ($ThCr_2Si_2$-type) and Fe_3Si (Au_3Cu-type) left unidentified peaks that could not be indexed with the tetragonal type of structure $ThMn_{12}$ which is adopted by UFe_9Si_3,[28] indicating that the third phase, UFe_5Si_3, possesses a different crystal structure. Several samples with initial composition UFe_5Si_3 were then synthesized by the classical arc-melting technique and heat-treated at various temperatures. The samples annealed at a temperature below 1473 K contain the three phases UFe_2Si_2, Fe_3Si, and UFe_5Si_3 (see Figure 1), whereas those annealed above 1573 K contain only the phases UFe_2Si_2 and Fe_3Si, suggesting that UFe_5Si_3 is formed by a peritectoid reaction between UFe_2Si_2 and Fe_3Si at a temperature in the range 1473−1573 K. No further characterization was attempted to determine precisely the exact nature and temperature of formation of UFe_5Si_3. Another important piece of information provided by these trials is that the typical synthetic route by means of arc-melting of the components followed by annealing does not yield a pure sample of UFe_5Si_3. To obtain pure samples of this new compound, only a rapid solidification of the melt, using the splat cooling technique followed by annealing at 1173 K, was successful.

Ab Inito Structure Determination and Rietveld Refinement. An examination of the X-ray diffraction pattern straightforwardly revealed the presence in the vicinity of 28.20° in 2θ of the (111) diffraction peak of UO_2 which was thus excluded in the following steps. Determination of the peak position was performed with the help of the program WinPLOTR. The automatic indexation was carried out with the program DICVOL04[29] taking into account the first 13 diffraction peaks. A tetragonal solution was found with unit-cell parameters very close to those obtained in the finale Rietveld refinement (see Table 2). The corresponding figures of merit of $M(13) = 178$;[30] $F(13) = 111.8$ (0.0055, 21)[31] were judged satisfactory, and a whole pattern profile refinement was then undertaken with the space group $P4$ which presents no systematic absence. A close examination of the indexed pattern showed that no conditions limiting possible reflections can be deduced, and therefore the structure determination of UFe_5Si_3 was carried about considering the highest symmetry for the primitive tetragonal space group, $P4/mmm$. The program FULLPROF was used to extract the factor structure intensities, and the structure determination was performed by direct methods with the EXPO package.[32] The crystallographic positions of the U atom and two Fe atoms were directly located, yielding a reliability factor R_f of 0.101. Position of the two silicon atoms was found through subsequent difference Fourier calculations ($F_{obs}-F_C$). Attempts to refine independently the isotropic displacements yield negative values for silicon atoms and therefore an overall temperature factor was used. Although the site occupancy is correlated to atomic displacement parameters, both the chemical analyses and the variation in powder cell parameters are consistent with a well-defined compound. Each crystallographic independent site is occupied by only one atom yielding a structural model of UFe_5Si_3 fully ordered. The final Rietveld refinement leads to the following reliability factors: $R_B = 6.32\%$; $R_p = 8.93\%$; $R_{exp} = 10.9\%$; $R_{wp} = 12.5\%$; and $\chi^2 = 1.32$ (see Table 2). The comparison between observed and the calculated pattern and the difference curve are shown in Figure 2. Crystallographic parameters, including the atomic positions and a selection of bonds along with the coordination polyhedra, are given in Tables 2 and 3, respectively.

Table 2. Rietveld Refinement and Atomic Coordinates of UFe_5Si_3

formula	UFe_5Si_3
space group	$P4/mmm$ (No. 123)
lattice parameters (Å)	$a = 3.9296(5)$
	$c = 7.7235(1)$
number of points	6449
total number of refined parameters	22
number of reflections	89
number of refined crystallographic parameters	5
profile function	Thompson-Cox-Hastings pseudo-Voigt
background function	refined manual background
overall temperature factor	0.12(3)
R factors (%)	$R_B = 6.32$
	$R_p = 8.93$
	$R_{exp} = 10.9$
	$R_{wp} = 12.5$
	$\chi^2 = 1.32$

atom	Wyckoff position	x	y	z
U	1c	0.5	0.5	0
Fe1	1b	0	0	0.5
Fe2	4i	0.5	0	0.3130(2)
Si1	2g	0	0	0.1543(5)
Si2	1d	0.5	0.5	0.5

Crystal Structure Description. The interatomic distances found in UFe_5Si_3 compare well those reported for all the

(28) Andreev, A. V.; Andreev, S. V.; Tarasov, E. N. *J. Less-Common Met.* **1991**, *167*, 255−259.
(29) Boutlif, A.; Louer, D. *J. Appl. Crystallogr.* **2004**, *37*, 724.
(30) de Wolff, P. M. *J. Appl. Crystallogr.* **1972**, *5*, 243.
(31) Smith, G. S.; Snyder, R. L. *J. Appl. Crystallogr.* **1979**, *12*, 60.
(32) Altomare, A.; Burla, M. C.; Camalli, M.; Carrozini, B.; Cascarano, G.; Giacovazzo, C.; Guagliardi, A.; Moliterni, A. G. G.; Polidori, G.; Rizzi, R. *J. Appl. Crystallogr.* **1998**, *32*, 339.

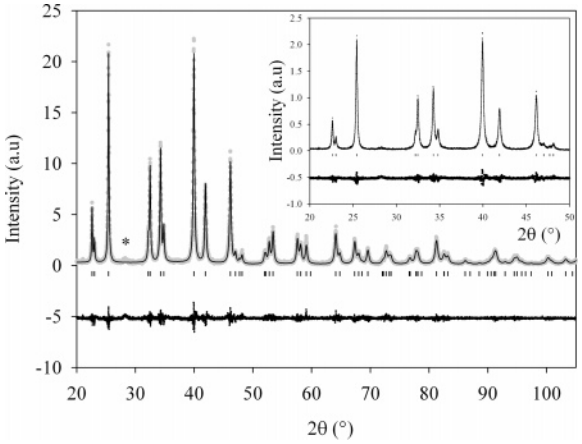

Figure 2. Observed (circles) and calculated (continuous line) data of the powder diffraction patterns of UFe_5Si_3. Vertical ticks are related to the Bragg angles positions in space group *P4/mmm*. The lower profile gives the difference between the observed and the calculated data. The inset gives the details of the 20−50° domain in 2θ. The black star shows the UO_2 impurity peak.

Table 3. Interatomic Distance (Å)[a]

atoms	coordinated atoms	distance (Å)
U	4 U	3.929(1)
	8 Si1	3.024(2)
	8 Fe2	3.115(1)
Fe1	8 Fe2	2.439(1)
	2 Si1	2.669(4)
	4 Si2	2.779(1)
Fe2	2 Si1	2.315(2)
	2 Si2	2.439(1)
	2 Fe1	2.439(1)
	4 Fe2	2.779(0)
	2 U	3.115(1)
Si1	4 Fe2	2.315(2)
	4 Si1	3.929(1)
	1 Fe1	2.669(4)
	1 Si1	2.383(1)
	4 U	3.024(2)
Si2	8 Fe2	2.439(1)
	2 Si2	3.929(1)
	4 Fe1	2.779(0)

[a] $r_U = 1.56$ Å, $r_{Fe} = 1.25$ Å, $r_{Si} = 1.18$ Å.

other ternary phases of the U−Fe−Si system and are consistent with the sum of the metallic radii (U = 1.56 Å, Fe = 1.25 Å) and covalent radius (Si = 1.18 Å). Remarkable contacts for an intermetallic compound are the short Fe−Si and Si−Si distances of 2.315(1) Å and 2.383(1) Å, indicating some degree of covalency in these bonds and the formation of Si2 dumbbells. Another interesting feature of the crystal structure is the Fe−Fe spacing of 2.438(1) Å, shorter that the inter-iron distance in the body-centered cubic metallic form (α form). However, even smaller bonding lengths have been observed in the ferromagnets $UFe_{10}Si_2$[5] and $U_2Fe_{17-x}Si_x$[17] crystallizing with the $ThMn_{12}$-type and Th_2Ni_{17}-type, respectively.

A perspective view of the UFe_5Si_3 structure which also outlines the short interatomic contacts is depicted in Figure 3. The structure of UFe_5Si_3 can be viewed as built up from an infinite three-dimensional framework of Fe and Si atoms, which define tunnels with a hexagonal section where the U atoms lie. The U atom shows a typical coordination number of 20, composed of 8 Fe atoms and 8 Si atoms, each element building a square prism, and by 4 additional U atoms in the basal (*a*, *b*) plane. Similar coordination polyhedron around

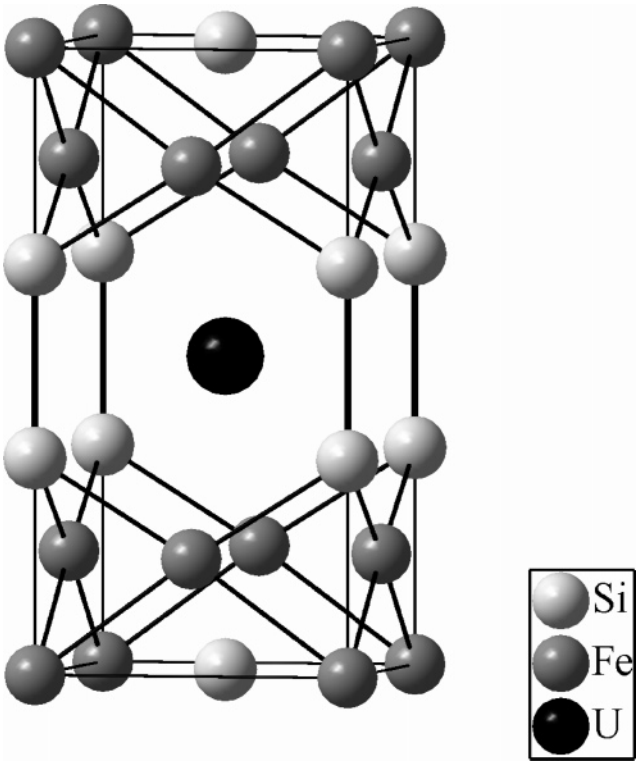

Figure 3. Perspective view of the crystal structure of UFe_5Si_3. Thick black lines correspond to the Si−Si, Si−Fe, and Fe−Fe bonds, emphasizing the Fe−Si tridimensional framework.

the U atom is encountered for the ternary compounds crystallizing with the well-known body-centered tetragonal $ThCr_2Si_2$ type with the space group *I4/mmm*. The ternary UFe_2Si_2 compound crystallizes with this structural model,[33] which consists of basal planes of U, Fe, and Si atoms, respectively, stacked along the *c*-axis with the sequence U−Si−Fe−Si−U−Si−Fe−Si forming a natural multilayer. The increase of the dimensionality from two-dimensional in UFe_2Si_2 to three-dimensional in UFe_5Si_3 is a direct consequence of lower uranium content. The 5f element can transfer less electron density toward the iron and silicon atoms, as a result the dimensionality of the [Fe × Si_y] network rise, as recently observed for the compound $Yb_2Ru_3Ge_4$.[34]

Although the composition UT_5Si_3 (T is a 3d transition metal) is quite common in the crystal chemistry of ternary uranium silicides (compounds with T = Ni and Co exist), UNi_5Si_3[35] and UCo_5Si_3[36] each crystallize with a different atomic arrangement and no simple relationship can be drawn between these two structures and the model of UFe_5Si_3. Instead, the crystal structure of UFe_5Si_3 bears strong resemblance with the $BaCu_6P_2$-type.[37] Both UFe_5Si_3 and $BaCu_6P_2$ crystallize in the tetragonal system with space group *P4/mmm*, with the atoms located on the same crystallographic sites. The main difference is that the 1c Wyckoff position is

(33) Ban, Z.; Sikirica, M. *Z. Anorg. Allg. Chem.* **1967**, *356*, 96−104.
(34) Schappacher, F. M.; Katoh, K.; Pöttgen, R. *J. Solid State Chem.* **2007**, *180*, 185−189.
(35) Aksel'rud, L. G.; Yarovets, V. I.; Bodak, O. I.; Yarmolyuk, Ya. P.; Gladyshevskii, E. I. *Sov. Phys. Kristallogr.* (translated from *Kristallografiya*) **1976**, *21*, 210.
(36) Yarmolyuk, Ya. P.; Aksel'rud, L. G.; Fundamenskii, V. S.; Gladyshevskii, E. I. *Sov. Phys. Kristallogr.* (translated from *Kristallografiya*) **1978**, *23*, 531−533.
(37) Dünner, J.; Mewis, A. *J. Alloys Compd.* **1995**, *221*, 65−69.

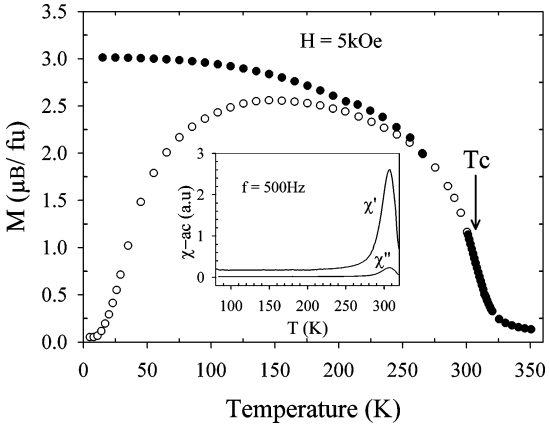

Figure 4. Temperature-dependent magnetization of free powder of UFe_5Si_3 under an applied field of 5 kOe performed on ZFC (filled circle) and FC (open circle) modes in the temperature range 5−350 K. The inset shows the temperature dependence of the real (χ') and imaginary (χ'') components of the ac susceptibility for free powder of UFe_5Si_3.

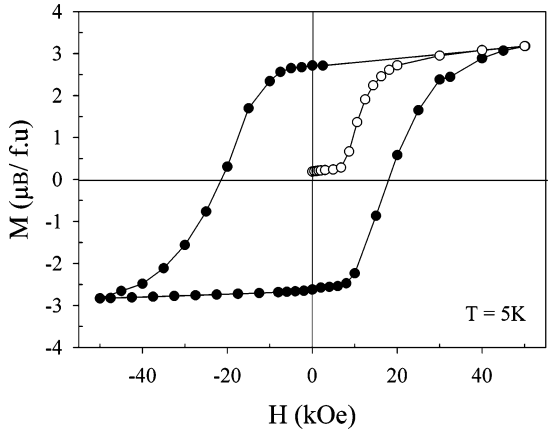

Figure 5. Hysteresis loop (filled circle) and initial magnetization curve (open circle) for UFe_5Si_3, performed on free powder at 5 K.

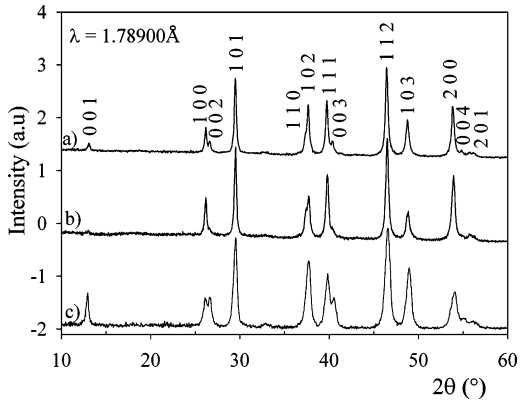

Figure 6. X-ray powder diffraction patterns of UFe_5Si_3, along with the indexation of the diffracted peaks (a) randomly oriented, (b) magnetically oriented by an applied field parallel to the plane of diffraction, and (c) magnetically oriented by an applied field perpendicular to the plane of diffraction.

occupied by a silicon atom in the silicide whereas it is occupied by a copper atom in the phosphide. More surprising is to find the quinary oxide $YBa(Cu_{1.10}Co_{0.90})O_5$[38] presenting the same crystallographic parameters (system, space group), with atoms located on the Wyckoff positions 1a, 1c, 1d, 2h, and 4i.

Magnetic Properties. The temperature dependence of the dc magnetization of UFe_5Si_3 performed on free powder under an applied field of 5000 Oe, both for ZFC and FC modes, is shown in Figure 4. The pronounced difference in the low field magnetization of ZFC and FC features a ferromagnet with strong magnetocrystalline energy. Such thermomagnetic irreversibility may arise when the anisotropy energy is comparable to the exchange energy leading to domains with narrow walls and high intrinsic coercive field. The phenomenon, which is observed for most of the U-based ferromagnetic compounds, vanishes either when a sufficient field is applied or when a certain temperature is reached. To precisely determine the value of the Curie temperature, ac-susceptibility measurements have been carried out. It is seen in inset of Figure 4 that both real $\chi'(T)$ and imaginary $\chi''(T)$ components show a sharp maximum at a temperature of 310 K, indicating long-range magnetic ordering in agreement with the ferromagnetic behavior of UFe_5Si_3 deduced from the dc magnetization. Below 250 K $\chi'(T)$ and $\chi''(T)$ remain flat and parallel indicating that no spin reorientation occurs between T_c and 80 K.

The hysteresis loop measured at 5 K (Figure 5) clearly indicates a hard ferromagnetic behavior. The initial magnetization curve increases sharply above 8 kOe with increasing magnetic field and fully saturates above 25 kOe, yielding a saturation moment of about 3 μB per formula unit. Upon decreasing the applied field, the magnetization remains almost constant, yielding a value of remanent magnetization of about 2.7 μB per formula unit. The hysterisis loop displays a substantial coercive field of Hc = 17 kOe, which confirms a high magnetic anisotropy in this compound. The significant slope above $H = 25$ kOe indicates that the saturation is not attained at 5 K up to 50 kOe when the sample is magnetized. This observation and the absence of anomaly below T_c in ac and dc magnetic measurements suggest that the ferromagnetic components are strongly confined along a peculiar crystallographic axis in this compound.

Figure 6 displays the x-ray diffraction patterns, of powder randomly oriented along with the *hkl* indexation of the peaks (fig. 6-a), and of powder magnetically oriented by applying a field parallel (fig. 6-b) and perpendicular to the plane of diffraction (fig. 6-c). On the diffractogram with the field parallel to the diffraction plane, a significant decrease is observed, up to the vanishing of the intensity of the 00*l* peaks and an increase of the intensity of the *hk*0 peaks, especially the 100, 110, and 200 reflections. On the diffractogram with the applied field perpendicular to the diffraction plane, an opposite situation is noticed, the intensity of 00*l* peaks considerably rises up, whereas the intensity of the *hk*0 peaks scales down. Despite the weak alignment of the powder, performed at a temperature in the vicinity of the magnetic transition, this points out that the majority of the crystallites have their *c*-axes parallel to each other in the oriented samples, revealing strong indications for a uniaxial magnetocrystalline anisotropy, with the *c*-direction as the easy axis.

The magnetization $M_{\parallel}$ and $M_{\perp}$ measured at 5 K as a function of magnetic field applied parallel and perpendicular to the crystallographic *c*-axis, respectively, are depicted in

(38) Gainsford, G. J.; Tallon, J. L.; Lin, C. T. *Acta Crystallogr., Sect. C* **1997**, *53*, 1729−1730.

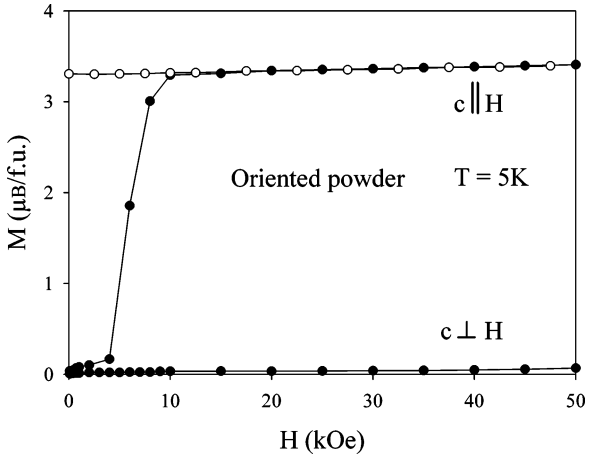

Figure 7. Isothermal magnetization of UFe_5Si_3 at 5 K as a function of magnetic field applied parallel and perpendicular to the *c*-axis measured with increasing (filled circles) and decreasing (open circles) magnetic field.

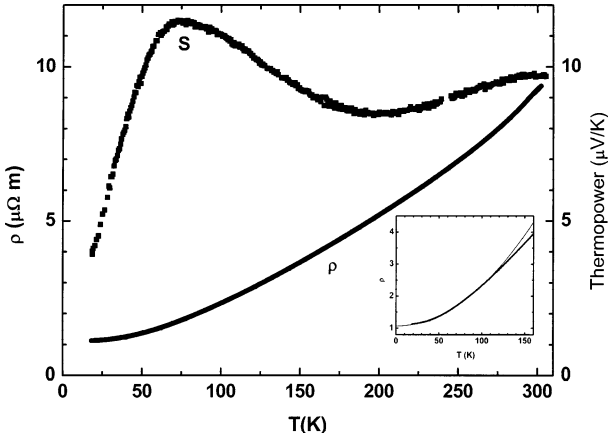

Figure 8. Temperature dependencies of the electrical resistivity and thermoelectric power of UFe_5Si_3 performed in the temperature range 18−300 K on the bulk sample. Inset: fit of the low-temperature region according to the Fermi liquid law $\rho = \rho_0 + AT^2$.

Figure 7. $M_\perp$ is very small and shows linear field dependence. In contrast, $M_{||}$ initially increases linearly with applied field up to 4 kOe at which the magnetization increases sharply and fully saturates at about 10 kOe. The temperature dependence of $M_{||}$ reveals a typical behavior for a strong uniaxial anisotropy, which arises from a considerable magnetic moment of the U sublattice. For applied field above 15 kOe, $M_{||}$ remains constant, proving equal saturation moment (μsat) and spontaneous magnetic moment (Ms) of 3.3 μB per formula unit. Although this value has a large uncertainty, as a result of the rough estimation of the amount of oriented powder (about a few milligrams), it is much smaller that the saturation moment $\mu_{sat} = 2.23$ μB per Fe and $\mu_{sat} = 3.2$ μB per U^{4+} estimated in the Russel−Saunder model ($\mu_{sat} = gJ\,\mu$B). However, this humble value compares well those reported for the binary UFe_2[1,2] or ternary uranium and iron compounds such as $UFe_{10}Si_2$,[9] $U_2Fe_{14.6}Si_{3.4}$,[39] and $UFe_{12}Al_5$,[15] which exhibit magnetic contribution on both the uranium and iron sublattices. In UFe_5Si_3, the strong uniaxial anisotropy, the low value of the spontaneous magnetization, and the relatively high Curie temperature give strong evidence of significant magnetic contributions of both the U and the Fe sublattices. Unfortunately, attempts to synthesize an UFe_5Si_3 analogue by substituting U by a nonmagnetic element such as Y, to estimate the U magnetic contributions, were unsuccessful.

Figure 8 shows the temperature dependence of both the electrical resistivity ($\rho(T)$) and thermoelectric power ($S(T)$) of UFe_5Si_3 measured on bar-shaped samples cut from the annealed disc. The curve of the resistivity has a metallic character with a value of about 10 $\mu\Omega$·m at room temperature. As the temperature decreases, $\rho(T)$ decreases monotonously to reach of value of about 1 $\mu\Omega$·m at 18 K. No anomaly featuring another magnetic transition is observed below 300 K. The temperature variation of the electrical resistivity of UFe_5Si_3 has the typical shape expected for a ferromagnetic material. The data follow the Fermi liquid law $\rho = \rho_0 + AT^2$, as expected in a ferromagnetic phase, up to 110 K (see inset of Figure 8). The residual resistivity ρ_0 takes the value $\rho_0 = 1.069(2)$ $\mu\Omega$·m, and the constant value A amounts to $A = 1.236(2) \times 10^{-4}$ $\mu\Omega$·m·K^{-2}. The measurement of the thermoelectric power indicates modest values of a few μV/K in line with the metallic behavior of UFe_5Si_3. The shape of $S(T)$ is characterized by a smooth decrease down to 180−200 K followed by a broad maximum around 60 K and finally by a rapid fall at the lowest temperature. The thermopower measurement, which is a sensitive method to illustrate the competing interaction present in a heavy-fermion system,[40,41] may indicate weak Kondo scattering and/or crystal electrical field (CEF) effect at low temperature. However, such an anomaly at about 60 K can be definitively ascribed to 5f electrons of uranium, indicating that the Fe 3d−U 5f hybridization is not integral, but some 5f electron density remains on uranium atoms.

Conclusion

The new ternary compound UFe_5Si_3 was synthesized by rapid solidification of the melt followed by annealing at 1173 K for 10 days. Comparison between as-cast and heat-treated samples of the exact composition suggest a peritetoid formation from $UFe_2Si_2 + Fe_3Si \rightarrow UFe_5Si_3$ at a temperature not precisely determined but estimated in the range 1473−1573 K. Its crystal structure determined by X-ray diffraction on powder revealed an original atomic arrangement in the tetragonal space group *P*4/*mmm*, with unit-cell parameters $a = 3.9298(3)$ Å and $c = 7.7133(6)$ Å. Magnetic measurements carried out on free and oriented powder indicate a ferromagnetic behavior with a strong uniaxial anisotropy confined to the *c*-axis. The low value of the saturation moment suggests a strong hybridization between the iron 3d electrons and the uranium 5f electrons. No spin reorientation can be detected on the thermal variation of both the ac susceptibility and electrical resistivity. However, evidence of electronic perturbations is revealed on the thermal variation of the thermopower as a maximum around 60 K which can be ascribed to effects on the U 5f electrons due to crystal field or Kondo screening.

(39) Andreev, A. V.; Nižňanský, D.; Homma, Y.; Onodera, H.; Shiokawa, Y.; Satoh, I. *Physica B* **2005**, *369*, 100−103.
(40) Bhattachajee, A. K.; Coqblin, B. *Phys. Rev. B* **1976**, *13*, 3441.
(41) Amato, A.; Jaccard, D.; Sierro J.; Lapierre, F.; Haen, P.; Lejay, P.; Flouquet, J. *J. Magn. Magn. Mater.* **1988**, *76*−*77*, 263.

Acknowledgment. We thank Dr. M. Ceretti, Dr. O. Hernandez, and Dr. T. Roisnel for their contributions to the X-ray diffraction data collection and helpful advice in the Rietveld refinements, respectively. This work was partially supported by the PESSOA/GRICES Project 2007-2008 No. 14729NF.

Supporting Information Available: Crystallographic data in CIF format. This material is available free of charge via the Internet at http://pubs.acs.org.

CM070943W